Effects of L-Phenylalanine as a Nucleation Agent on the Nonisothermal Crystallization, Melting Behavior, and Mechanical Properties of Poly(3-hydroxybutyrate-*co*-3-hydroxyhexanoate)

Rongcong Luo, Kaitian Xu, Guoqiang Chen

Multidisciplinary Research Center, Shantou University, Shantou, Guangdong 515063, China

Received 26 September 2007; accepted 6 February 2008
DOI 10.1002/app.28240
Published online 3 September 2008 in Wiley InterScience (www.interscience.wiley.com).

ABSTRACT: Poly(3-hydroxybutyrate-*co*-3-hydroxyhexanoate) (PHBHHx) is a thermoplastic biopolyester with a slow crystallization rate. L-Phenylalanine (L-PH) was used to improve the crystallization rate of PHBHHx. The nonisothermal crystallization kinetics and melting behaviors of PHBHHx and PHBHHx/L-PH samples were characterized and compared with differential scanning calorimetry. At cooling rates of 2, 5, 10, and 20°C/min, PHBHHx/L-PH could crystallize at higher temperatures than pure PHBHHx. A modified Avrami equation based analysis showed that the addition of L-PH shortened the half-time of crystallization of PHBHHx from 9.6 to 8.0 min and increased the composite rate constant of PHBHHx from 0.201 to 0.283 during the nonisothermal crystallization process at a cooling rate of 10°C/min. For other cooling rates, similar trends of changes were observed. These indicated a faster crystallization rate of PHBHHx in the presence of L-PH. PHBHHx/L-PH samples showed a higher melting temperature and a sharper melting peak than those of the pure PHBHHx, which suggested that L-PH as a nucleation agent improved the perfection of the PHBHHx crystals. Stress–strain measurements showed that both PHBHHx and PHBHHx/L-PH maintained their ductile and elastic properties during the 60 days of the aging study. © 2008 Wiley Periodicals, Inc. J Appl Polym Sci 110: 2950–2956, 2008

Key words: biopolymers; blending; crystallization; films

INTRODUCTION

Polyhydroxyalkanoates (PHAs) are a family of polyesters accumulated by a variety of microorganisms as intracellular energy and carbon-source reserve materials.[1] Because of their biocompatibility, biodegradability and renewable source origins, PHAs have been considered environmentally friendly plastics.[2] Among the PHA family, poly(3-hydroxybutyrate) (PHB) and poly(3-hydroxybutyrate-*co*-3-hydroxyvalerate) (PHBV) have been produced on a commercial scale.[3] However, the application of PHB is restricted by its intrinsically high crystallinity and thermal instability.[4] To overcome these shortcomings, the copolymerization of 3-hydroxybutyrate (3HB) with other hydroxyalkanoates (HAs) such as 3-hydroxypropinoate, 4-hydroxybutyrate, and 3-hydroxyhexanoate (3HHx) have been successfully carried out with microbial fermentation to form copolyesters such as PHBV, poly(3-hydroxybutyrate-*co*-4-hydroxybutyrate) (P3HB4HB), and poly(3-hydroxybutyrate-*co*-3-hydroxyhexanoate) (PHBHHx), respectively.[3,5,6]

PHBHHx produced on a large scale by *Aeromonas* strains is a random copolymer containing both short-chain-length HB monomer and medium-chain-length 3HHx monomer.[7] Depending on the 3HHx content, the biodegradation, mechanical, and thermal properties of PHBHHx are adjustable.[7] PHBHHx containing 10–17 mol % 3HHx fractions was reported to possess similar mechanical properties to low-density polyethylene and showed much better elongation at break values than PHBV containing 20 mol % 3-hydroxyvalerate.[6] Furthermore, PHBHHx containing 12 mol % 3HHx accumulated by *Aeromonas hydrophila* 4AK4 was widely investigated as a promising tissue engineering material.[8,9] *A. hydrophila* 4AK4 isolated from wastewater can accumulate PHBHHx with 12–15 mol % 3HHx when grown in an excess carbon source such as dodecanoic acid under the limitation of growth essential elements such as phosphate, sulfur, and nitrogen.

However, the crystallization rate of PHBHHx is slow.[6,10] Thus, PHBHHx remains sticky for a long time after it is cooled from the melt extruder, which

Correspondence to: K. Xu (ktxu@stu.edu.cn) or G. Chen (chengq@stu.edu.cn).

Contract grant sponsor: Li Ka Shing Foundation.
Contract grant sponsor: National Science Foundation of China; contract grant number: 20474001 (to K.X.).
Contract grant sponsor: National High Tech Project 863; contract grant number: 2006AA02Z242 (to G.C. and K.X).

© 2008 Wiley Periodicals, Inc.

leads to some difficulties for its melt processing. Furthermore, the slow crystallization rate of a polymer will result in secondary crystallization, which deteriorates the mechanical properties of the mold products when the polymer is used at room temperature for longer periods of time.[11,12]

An effective way to enhance the crystallization rate of a polymer is the addition of nucleation agents. Traditional nucleation agents, including boron nitride (BN), talc, and terbium oxide (Tb_2O_3), have found application in the processing of many polymers.[13] Besides the traditional nucleation agents, some other components from biosources have also been investigated as nucleation agents and have found positive effects. Kai et al.[14] added lignin particles to PHB and investigated their isothermal and nonisothermal crystallization processes; they found that lignin particles shortened the crystallization half-time ($t_{1/2}$) of PHB. Ke and Sun[15] extruded poly (lactic acid) and starch blends. They found that the blending component starch could accelerate the crystallization of poly(lactic acid), and it was comparable with the efficiency of the BN. He et al.[16] used α-cyclodextrin to enhance the crystallization of PHB. They found that α-cyclodextrin improved the crystallization of PHB greatly. Subsequently, Dong et al.[17] investigated the nucleation effects of α-cyclodextrin and its inclusion complexes (ICs) with poly(ε-caprolactone), poly(ethylene glycol), and poly(butylenes succinate) on the crystallization rate of these polymers. They demonstrated that the IC of a given polymer could greatly enhance the nucleation and crystallization of the polymer itself. ICs are defined to have a host–guest molecular structure. A typical example for the host molecule is a cyclodextrin. Cyclodextrins can complex and include water-insoluble polymers into their channel structure to form ICs. One explanation for the ICs enhancing the crystallization rate of a polymer is that the molecular chains of a polymer such as PHB included in the cyclodextrin channel structure were less entangled and highly extended. The ordered structure of the molecular chains benefits the crystallization rate.[17,18]

This study aimed to improve the crystallization behaviors of PHBHHx with a biodegradable and biocompatible nucleation agent to allow the biopolyester to be used in tissue engineering. However, traditional nucleation agents are nonbiodegradable; some of them are even toxic.[13] We selected a crystal amino acid, L-phenylalanine (L-PH), as the nucleation agent for PHBHHx with the hope of improving the crystallization rate of PHBHHx. L-PH is a crystal aromatic amino acid with a melting point of 283°C. It is one of the essential amino acid for animals, and it is converted to tyrosine *in vivo*. To our knowledge, this is the first time a crystal amino acid has been selected as a nucleation agent for a polymer.

EXPERIMENTAL

Materials

PHBHHx containing 13.5 mol % 3-HHx was provided by Procter & Gamble (Cincinnati, OH). Its number-average molecular weight was 320,000, and its polydispersity (weight-average molecular weight/number-average molecular weight) was 1.75, as revealed by gel permeation chromatography (Waters 1525, Waters Corp., USA). To eliminate contaminants that may have acted as potential nucleation agents, we dissolved PHBHHx in hot chloroform, filtrated it to remove insoluble particles, and then precipitated the polymer by addition of ice-cold absolute ethanol.

L-PH was purchased from Sigma–Aldrich (Shanghai, China) and was used as received. The L-PH crystal granules were grounded into fine powders and sieved through a 270-mesh/in. sieve to obtain homologous sized particles.

Blend preparation

PHBHHx and L-PH powders were thoroughly blended at a weight ratio of 99 : 1. A high-speed blender (HB-200 Aifeng Technical Group, Shanghai, China) was used to blend these two components. The blends were pressed to form film-shaped samples between two stainless steel sheets at 120°C for 4 min under a pressure of 5 MPa with a mechanical presser (VP-40, YEE SEN Industrial Group, Jinan, China). The two stainless sheets were quickly cooled in ice water to obtain amorphous polymer films. Finally, the films were stored at room temperature in a glass desiccator with silica to allow crystallization to proceed. All the films were maintained for 3 weeks at room temperature so they could reach crystallinity equilibrium before further studies. For the pure PHBHHx films, the same treatment process was applied.

Differential scanning calorimetry (DSC)

The nonisothermal crystallization studies of PHBHHx and PHBHHx/L-PH were carried out with a TA-Q100 differential scanning calorimeter (Thermal Analysis Corp., New Castle, DE). It was calibrated with an indium standard as indicated by the instrument manufacturer. Samples weighing 3–4 mg were heated to 120°C at 10°C/min. After they were maintained at 120°C for 1 min, the molten samples were cooled at rates of 2, 5, 10, and 20°C/min to −60°C. The crystallization enthalpy and peak crystallization temperature values were determined from the exothermal peak areas and values in the DSC cooling curve, respectively. Subsequently, the samples were reheated to 120°C to study their melting behaviors.

The melting temperature and heat of fusion were determined from the endothermal peak values and areas in the DSC heating process.

Stress–strain measurement

The stress–strain curves of PHBHHx and PHBHHx/L-PH films were recorded with a CMT-4000 universal testing machine (Shenzhen Sans Cooperation, Shenzhen, China) at room temperature. The samples were cut into dumbbell-shaped specimens with a width of 4 mm and a thickness of approximately 300 μm. The speed of the crosshead was 5 mm/min. To study aging effects on the mechanical properties, stress–strain measurements were conducted after the films were aged for 1, 7, 30, and 60 days at room temperature.

RESULTS AND DISCUSSION

Nonisothermal crystallization characterization

Practical polymer processings, such as extrusion, molding, and film forming, usually occur under dynamic, nonisothermal crystallization conditions.[19] Therefore, it is important to evaluate the nonisothermal crystallization parameters through the study of the nonisothermal crystallization kinetics.

The DSC exothermal curves of PHBHHx and the PHBHHx/L-PH blends at various cooling rates were recorded [Fig. 1(a,b)]. For both the PHBHHx and PHBHHX/L-PH samples, the crystallization process began at a higher temperature at slower cooling rates [Fig. 1(a,b)]. This could be explained from the view of dynamic thermal process variation: the sample stayed at each temperature for a longer time when the samples were cooled at a lower cooling rate during DSC scanning. Therefore, nuclei formation and crystal growth of the PHBHHx molecular chains could occur at a higher temperature. In contrast, when the samples were cooled down faster, the motion of the PHBHHX molecular chains could not follow the cooling temperature, and crystallization only happened at lower temperatures.[18]

The crystallization temperature, as an indirect measure of the nucleation effects of L-PH, was obtained to explain the crystallization rate change [Fig. 1(a,b)]. Generally, at the same cooling rate, a higher crystallization temperature means a faster crystallization rate.[17]

The nucleating effects of L-PH on the crystallization of PHBHHx were evaluated [Fig. 1(a,b)]. At the same cooling rate, such as 20°C/min, the PHBHHx in the PHBHHx/L-PH blends crystallized at 62°C, whereas the pure PHBHHx only crystallized at 50°C. At the other cooling rates, similar trends in the crystallization temperature changes were also observed.

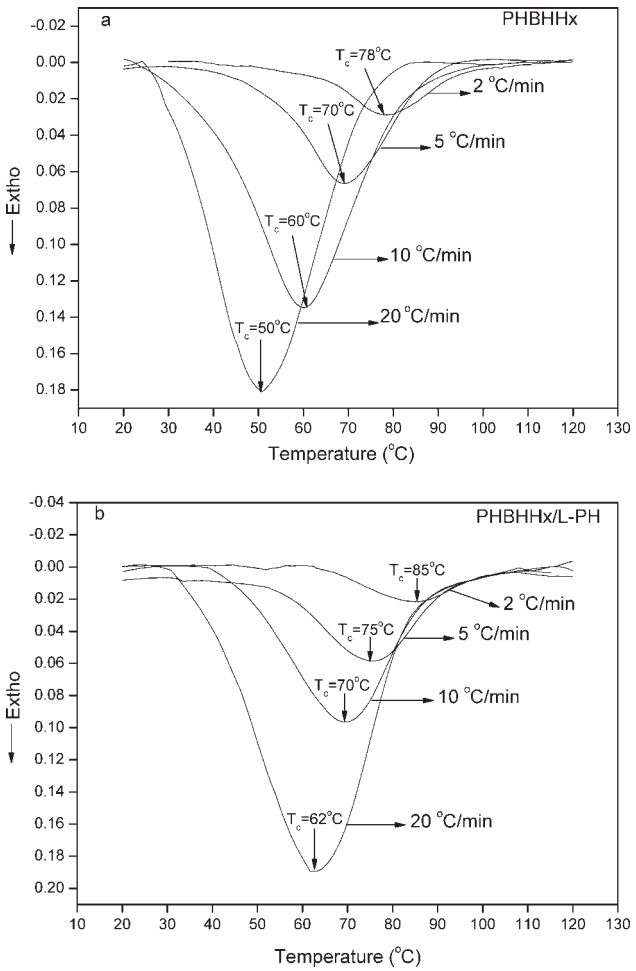

Figure 1 Exothermal crystallization peaks recorded from the cooling processes at different cooling rates: (a) pure PHBHHx nonisothermally crystallized at a cooling rate of 2, 5, 10, or 20°C/min and (b) PHBHHx/L-PH (99:1) nonisothermally crystallized at a cooling rate of 2, 5, 10, or 20°C/min (T_c is the crystallization temperature).

These results indicate that the addition of L-PH enhanced the crystallization rate of PHBHHx. According to Kai et al.,[14] the enhanced crystallization rate may have resulted from the reduced energy of the driving force for the polymer molecular chains in the nonisothermal crystallization process.

For the nonisothermal crystallization kinetic study, the relative crystallinity as a function of the crystallization temperature (X_t) was defined as follows:

$$X_t = \frac{\int_{T_o}^{T} \left(\frac{dH_c}{dT}\right) dT}{\int_{T_o}^{T_\infty} \left(\frac{dH_c}{dT}\right) dT} \quad (1)$$

where T_o and T_∞ are the temperatures at the onset and end of the crystallization process, respectively, and ΔH_c is the crystallization enthalpy. During the melt nonisothermal crystallization process, the

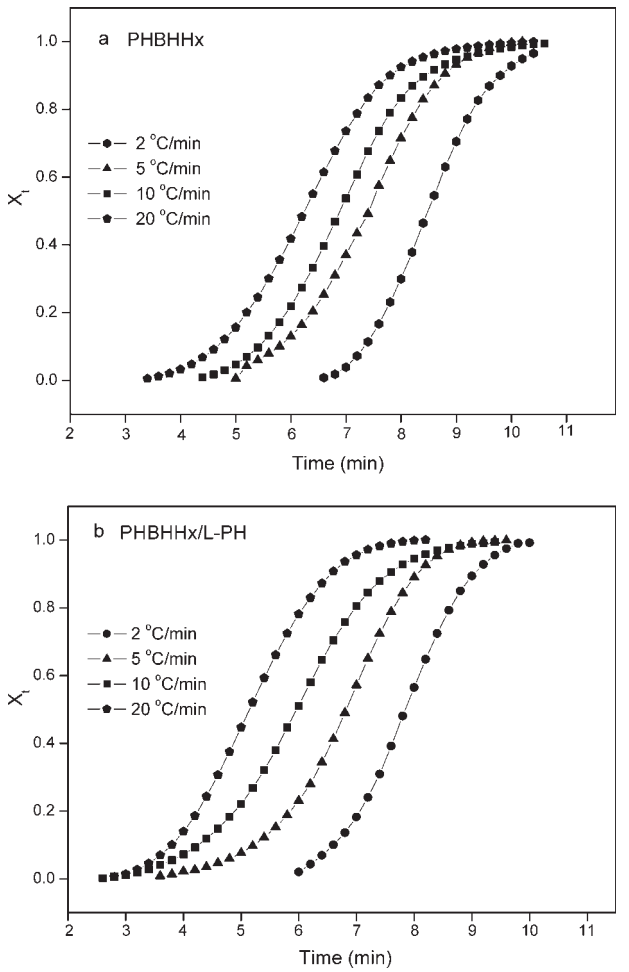

Figure 2 Development of the relative crystallinity degree (X_t) versus the crystallization time during the nonisothermal crystallization process: (a) pure PHBHHx and (b) PHBHHx/L-PH (99 : 1).

relation between the crystallization time (t) and the corresponding temperature (T) is given by

$$t = \frac{T_o - T}{\Phi} \tag{2}$$

where Φ is the cooling rate. It was 2, 5, 10, or 20°C/min.

According to eqs. (1) and (2), the temperature-dependent relative crystallinity can be transformed into the time-dependent relative crystallinity shown in Figure 2(a,b).

For both the pure PHBHHx and PHBHHx/L-PH samples, the higher the cooling rate was, the shorter the time was required for the completion of crystallization [Figs. 2(a,b)].

The widely accepted method for describing melt nonisothermal crystallization kinetics is again based on a modified Avrami equation[20] as follows:

$$1 - X_t = \exp(-Z_t t^n) \tag{3}$$

where the Avrami exponent (n) is a mechanism constant depending on the type of nucleation and growth process and Z_t is a composite rate constant involving both the nucleation and growth rate parameters.[14] However, the values of Z_t should be adequately corrected by consideration of the nonisothermal characters of the process investigated.[14] According to Jeziorny,[21] the factor to be considered is the cooling rate. Therefore, the final form of the parameter, characterization of the kinetics of the melt nonisothermal crystallization, is given as follows:

$$\log Z_c = \frac{\log Z_t}{\Phi} \tag{4}$$

where Z_c is the composite rate constant. According to eq. (3), the values of $\log[-\ln(1 - X_t)]$ were plotted against $\log t$ for both PHBHHx and PHBHHx/L-PH [Fig. 3(a,b)].

n and Z_c were determined from the slopes and intercepts of the lines [Fig. 3(a,b)], respectively. $t_{1/2}$ was also determined according to the equation $t_{1/2} = (\ln 2/Z_c)^{1/n}$ (Table I).

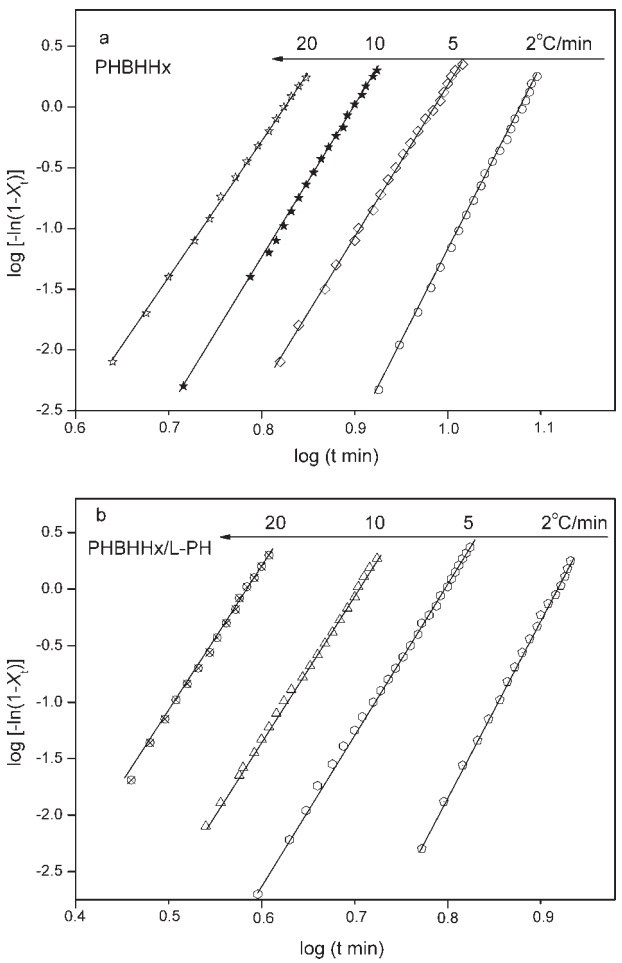

Figure 3 Nonisothermal crystallization kinetic curves recorded at different cooling rates: (a) pure PHBHHx and (b) PHBHHx/L-PH (99 : 1).

TABLE I
Values of n, Z_c, and $t_{1/2}$ for PHBHHx and PHBHHx/L-PH Crystallized Nonisothermally at Cooling Rates of 2, 5, 10, and 20°C/min

Sample	Cooling rate (°C/min)	n[a]	Z_c (min^{-1})[b]	$t_{1/2}$ (min)[c]
PHBHHx	2	3.75	0.121	11.5
	5	3.92	0.156	10.8
	10	4.15	0.201	9.6
	20	4.26	0.255	8.4
PHBHHx/L-PH (99 : 1)	2	4.05	0.20	10.2
	5	3.88	0.235	9.5
	10	4.22	0.283	8.0
	20	3.86	0.312	7.6

[a] Avrami exponent determined from the slope of the straight line drawn from the double-logarithm form of the modified Avrami equation.
[b] Composite rate constant determined from the intercept on the ordinate of the straight line drawn from the double-logarithm form of the modified Avrami equation.
[c] Half-time of crystallization defined as the time taken for 50% of the total crystallization volume of a PHBHHx or PHBHHx/L-PH sample.

The crystallization rates of both samples increased with increasing cooling rate, as indicated by the $t_{1/2}$ values [Fig. 3(a,b) and Table I]. The kinetic plots of PHBHHx and PHBHHx/L-PH were parallel to each other at each cooling rate, which indicated that the nucleation mechanism and crystal growth geometries were similar [Fig. 3(a,b)].

The values of $t_{1/2}$ for PHBHHx in the PHBHHx/L-PH were less than that of pure PHBHHx at each cooling rate (Table I). In contrast to the changes of the $t_{1/2}$ values, the general rate constant (Z_c) for PHBHHx/L-PH was lower than that of pure PHBHHx at each cooling rate (Table I). This suggested that the addition of the nucleation agent L-PH into the PHBHHx matrix increased the rate of crystalline phase formation and, thus, increased the overall crystallization rate.

At each cooling rate, the areas of the exothermal crystallization peaks of PHBHHx/L-PH were similar with those of pure PHBHHx. Usually, the change in the areas for the exothermal crystallization peaks can reflect a change in the crystallinity degree of a polymer. Consequently, the results in Figure 1 may demonstrate that the addition of L-PH into PHBHHx did not change the crystallization degree of PHBHHx.

Melting behavior

Pure PHBHHx sample exhibited a double melting peak [Fig. 4(a)], whereas the PHBHHx in PHBHHx/L-PH showed a single sharp melting peak in the first DSC heating process [Fig. 4(b)]. Double melting peaks generally relate to two factors; one is the different lamellar thicknesses, and the other is the existence of different types of crystals.[22] By increasing the heating rates to 20, 40, and 60°C/min, respectively, the double melting peak was observed to merge into one single melting peak (curves not shown), which implied that the double melting peak was the result of the existence of different lamellar thicknesses.[23,24] In addition, multiple melting peaks may also result from the recrystallization and reorganization process. Some polymers crystallized from the melt or glassy state exhibit two or three melting peaks. Generally, the lower melting peak is attributed to the melting of the preformed structure, and the higher one corresponds to the melting of the recrystallized fractions, which is due to the reorganization of the crystallites originally formed during the melting process.[25,26] According to Deng et al.,[27] double melting peaks also reflect a decrease in the lamellar thickness of a polymer. Therefore, when curves a and b were compared (Fig. 4), we con-

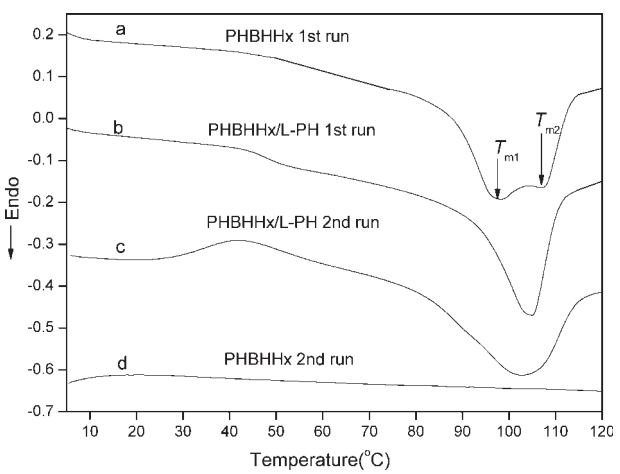

Figure 4 Melting behaviors recorded by the first DSC heating curve and second DSC reheating curve for the PHBHHx and PHBHHx/L-PH samples. For the second DSC reheating curve, the molten sample was quenched to −60°C, and the cooling rate was roughly estimated to be 100°C/min (T_{m1} and T_{m2} are the first and second melting temperatures, respectively).

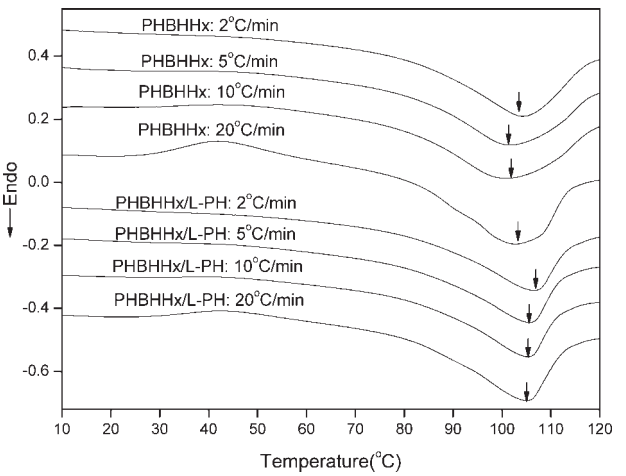

Figure 5 Melting behaviors recorded by the second DSC reheating curves for the PHBHHx and PHBHHx/L-PH samples cooled from the melt at various cooling rates.

cluded that L-PH helped accelerate the crystallization of PHBHHx and improved the perfection of the PHBHHx crystals when crystallization occurred at room temperature.

No melting peak was detected for the pure PHBHHx sample during the second DSC reheating curve after it was quenched to −60°C from the melt [Fig. 4(d)], which indicated the amorphous nature of the polymer in its reheating process. This phenomenon is generally observed for pure PHBHHx, P3HB4HB, and medium-chain-length PHA polymers.[28] These PHA polymers have a very low crystallization ability, and their molecular chains often fail to form the ordered structure for nuclei formation and crystal growth in the DSC reheating process after they are cooled from the melt, which is indicated by the disappearance of the melting peak [Fig. 4(d)]. On the other hand, PHBHHx in PHBHHx/L-PH had both the cold crystallization peak and the melting peak [Fig. 4(c)]. This suggested that PHBHHx in PHBHHx/L-PH had a better crystallization ability in the short DSC thermal history in the presence of the L-PH nucleation agent, which suggested that L-PH could not only accelerate the crystallization of PHBHHx in the high-temperature region shown here but also in the low-temperature region.

For both the PHBHHx and PHBHHx/L-PH samples cooled from the melt at various rates, a single melting peak was observed in the subsequent DSC heating curves (Fig. 5). However, two distinctly different features between the pure PHBHHx and PHBHHx/L-PH samples in the melting behaviors were distinguishable. They were the melting temperature and the shape of the melting peaks. PHBHHx in the PHBHHx/L-PH blends had higher melting peak temperature than that of pure PHBHHx at each cooling rate (Fig. 5). This phenomenon was similar with what Liu et al.[13] reported. They suggested that the better the nucleation effect is, the higher the melting point will be. At the same time, the peak shape of PHBHHx in the PHBHHx/L-PH blends was sharper than that of pure PHBHHx, which indicated a shorter time required for the completion of the melting process of the PHBHHx/L-PH sample. According to Liu et al.[13] and Dong et al.,[17] the sharper melting peaks indicate improved crystal perfection with a higher lamellar thickness of a polymer.

Mechanical behavior

Because of the slower crystallization rate of PHA polymers such as PHB and PHBV, PHA-based products continue to crystallize when used at room temperature. This is often described as the aging process of a polymer.[11] Aging is considered to be the result of a secondary crystallization process of a polymer. Secondary crystallization is believed to reduce the number of polymer chains in the amorphous phase, which results in a detrimental embrittlement of the materials.[11] Some methods can be used to reduce the secondary crystallization of a polymer, including the most common way, which is the addition of certain nucleation agents. Biddlestone et al.[11] compared the thermal and mechanical properties of pure PHBV and PHBV/BN samples, and they found that the PHBV added with BN as a nucleation agent exhibited much better antiaging properties than that of pure PHBV. The secondary crystallization phenomenon of PHBHHx was less obvious than those of PHB and PHBV.[29] The mechanical properties of the PHBHHx and PHBHHx/L-PH samples were studied and compared after the samples were aged at room temperature for 1, 7, 30, and 60 days, respectively (Fig. 6 and Table II). During the aging period, the tensile strength of PHBHHx and PHBHHx/

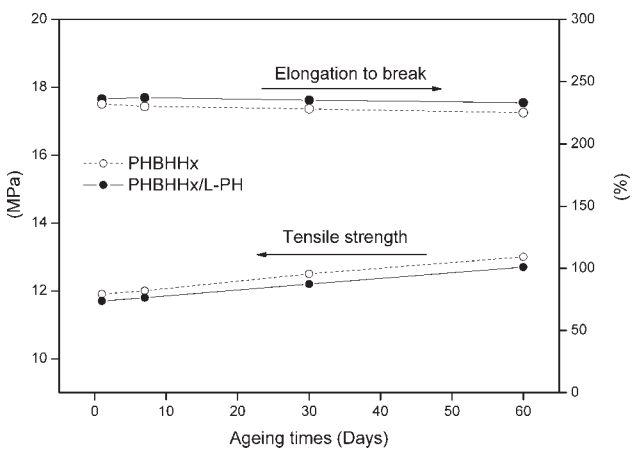

Figure 6 Tensile strength and elongation to break for the PHBHHx and PHBHHx/L-PH samples aged at room temperature for 1, 7, 30, and 60 days.

TABLE II
Effects of Aging on the Mechanical Properties of PHBHHx and PHBHHx/L-PH

Sample	Aging (days)	T (MPa)[a]	E (%)[b]
PHBHHx	1	11.8 ± 0.08	226 ± 0.75
	7	12 ± 0.11	226.5 ± 0.68
	30	12.5 ± 0.07	225 ± 0.53
	60	12.8 ± 0.05	225 ± 0.77
PHBHHx/L-PH	1	11.7 ± 0.1	226 ± 0.82
	7	12 ± 0.15	226.5 ± 0.77
	30	12.3 ± 0.17	225.5 ± 0.62
	60	12.7 ± 0.11	225 ± 0.83

[a] Tensile strength (MPa).
[b] Elongation at break (%).

L-PH increased slightly, whereas the elongation at break remained almost unchanged. In addition, the changes in stress–strain of the PHBHHx/L-PH sample were similar with that of pure PHBHHx at each aging time. The results suggest that both PHBHHx and PHBHHx/L-PH did not show aging behaviors when they were stored at room temperature, and the addition of the L-PH nucleation agent had little impact on the secondary crystallization behaviors and antiaging ability of PHBHHx. This may be explained by the nature of the low crystallization degree of PHBHHx and the defeated effect of the 3HHx monomer.[30,31] Because of the initial low crystallization degree of PHBHHx, the small amount of crystals developed by the secondary crystallization were nearly negligible in the rich amorphous phase of PHBHHx. Furthermore, the longer side chains of the noncrystallizable 3HHx unit were supposed to entangle with each other. On the other hand, the crystallization of 3HB only led to a small number of tiny crystals during the aging process, which should have not proceeded to enlarge further.

In summary, L-PH increased the crystallization rate of PHBHHx. 3HHx monomers restricted the increase in lamellar thickness of the PHBHHx crystals, regardless of the presence of L-PH, which helped to maintain a rich amorphous phase in the polymer, and thus, it retained its ductile and elastic properties for at least the 60 days tested in this study.

CONCLUSIONS

In the nonisothermal crystallization process, the faster the cooling rate was, the shorter the time was required for completion of crystallization for both PHBHHx and PHBHHx/L-PH. At each cooling rate (2, 5, 10, and 20°C/min), the addition of L-PH into PHBHHx helped to shorten the $t_{1/2}$ values, which indicated a faster crystallization rate in the PHBHHx/L-PH sample.

After the samples were quenched from the melt, no melting peak was detected for pure PHBHHx, whereas a clear melting peak was detectable for PHBHHx/L-PH. For samples cooled from the melt at different cooling rates, PHBHHx/L-PH showed a higher and shaper melting peak than that of pure PHBHHx, which indicated better crystal perfection in the PHBHHx/L-PH sample.

Both pure the PHBHHx and PHBHHx/L-PH samples showed little mechanical property change when they were stored at room temperature for 60 days.

References

1. Anderson, A. J.; Dawes, E. A. Microbiol Rev 1990, 54, 450.
2. Inoue, Y.; Yoshie, N. Prog Polym Sci 1992, 17, 571.
3. Cao, A.; Kasuya, K.-T.; Abe, H.; Doi, Y.; Inoue, Y. Polymer 1998, 39, 4801.
4. Barham, P. J.; Kellar, A. J Polym Sci Part B: Polym Phys 1986, 24, 69.
5. Kunioka, M.; Nakamura, Y.; Doi, Y. Polym Commun 1988, 29, 174.
6. Doi, Y.; Kitamura, S.; Abe, H. Macromolecules 1995, 28, 4822.
7. Chen, G. Q.; Zhang, G.; Park, S. J.; Lee, S. Y. Appl Microbiol Biotechnol 2001, 57, 50.
8. Deng, Y.; Zhao, K.; Zhang, X. F.; Hu, P.; Chen, G. Q. Biomaterials 2002, 23, 4049.
9. Chen, G. Q.; Wu, Q. Biomaterials 2005, 26, 6565.
10. Lim, J. S.; Noda, I.; Im, S. S. J Polym Sci Part B: Polym Phys 2006, 44, 2852.
11. Biddlestone, F.; Harris, A.; Hay, N. J.; Hammond, T. Polym Int 1996, 39, 221.
12. de Koning, G. J. M.; Lemstra, P. J. Polymer 1993, 34, 4089.
13. Liu, W. J.; Yang, H. L.; Wang, Z.; Dong, L. S.; Liu, J. J. J Appl Polym Sci 2002, 86, 2145.
14. Kai, W. H.; He, Y.; Naoki, A.; Yoshio, I. J Appl Polym Sci 2004, 94, 2466.
15. Ke, T. Y.; Sun, X. Z. J Appl Polym Sci 2003, 89, 1203.
16. He, Y.; Inoue, Y. Biomacromolecules 2003, 4, 1865.
17. Dong, T.; He, Y.; Zhu, B.; Shin, K. M.; Inoue, Y. Macromolecules 2005, 38, 7736.
18. Wei, M.; Shuai, X. T.; Tonelli, A. E. Biomacromolecules 2003, 4, 783.
19. An, Y. X.; Li, L. X.; Dong, L. S.; Mo, Z. S.; Feng, Z. L. J Polym Sci Part B: Polym Phys 1999, 37, 443.
20. (a) Avrami, M. J Chem Phys 1939, 7, 1103; (b) Avrami, M. J Chem Phys 1940, 8, 212; (c) Avrami, M. J Chem Phys 1941, 9, 177.
21. Jeziorny, A. Polymer 1978, 19, 1142.
22. Pearce, R.; Marchessault, R. H. Polymer 1994, 35, 3990.
23. Pearce, R. P.; Marchessault, R. H. Macromolecules 1994, 27, 3869.
24. Ishida, K.; Inoue, Y. Biomacromolecules 2004, 5, 1135.
25. Ji, X. L.; Zhang, W. J.; Wu, Z. W. J Polym Sci Part B: Polym Phys 1997, 35, 431.
26. Yasuniwa, M.; Tsubakihara, S.; Sugimoto, Y.; Nakafuku, C. J Polym Sci Part B: Polym Phys 2004, 42, 25.
27. Deng, X. M.; Hao, J. Y.; Yuan, M. L.; Xiong, C. D.; Zhao, S. J. Polym Int 2001, 50, 37.
28. Noda, I.; Satkowski, M. M.; Dowrey, A. E.; Marcott, C. Macromol Biosci 2004, 4, 269.
29. Asrar, J.; Valentin, H. E.; Berger, P. A.; Tran, M.; Padgette, S. R.; Garbow, J. R. Biomacromolecules 2002, 3, 1006.
30. Alata, H.; Aoyama, T.; Inoue, Y. Macromolecules 2007, 40, 4546.
31. Xu, J.; Guo, B. H.; Zhang, Z. M.; Zhou, J. J.; Jiang, Y.; Yan, S.; Lin, L.; Wu, Q.; Chen, G. Q.; Schultz, J. M. Macromolecules 2004, 37, 4118.